phys. stat. sol. (a) **73**, 475 (1982)

Subject classification: 1 and 18.2; 18.4; 21.4; 21.6

*Laboratoire Louis Néel, C.N.R.S., Grenoble*[1]) *(a),*
*Departamento Fisica Fundamental, Facultad de Ciencias, Universidad de Santander*[2]) *(b),*
*and Laboratoire de Diffraction Neutronique, D.R.F., Grenoble*[3]) *(c)*

# Magnetic Properties and Structure of $Tb_2Pt$

By

A. CASTETS (a), D. GIGNOUX (a), J. C. GOMEZ-SAL (b),
F. RODRIGUEZ-GONZALEZ (b), and E. ROUDAUT (c)

The magnetic properties and structure of polycrystalline $Tb_2Pt$ samples are studied. Below their Curie temperatures ($T_C = 98$ K) they exhibit ferromagnetic behaviour. The magnetic cell is identical to the crystallographic one. On terbium sites the ferromagnetic component is associated with an antiferromagnetic one. The magnetic structure is then non collinear and originates from the strong magnetocrystalline anisotropy which, in such compounds with low symmetry, determines a moment direction which is different from one atom to the other. This strong anisotropy leads at low temperature to narrow wall between magnetic domains.

Die magnetischen Eigenschaften und die Struktur von polykristallinen $Tb_2Pt$-Proben werden untersucht. Unterhalb der Curie-Temperatur ($T_C = 98$ K) zeigen sie ferromagnetisches Verhalten. Die magnetische Einheitszelle ist mit der kristallographischen identisch. Auf Terbiumplätzen ist die ferromagnetische Komponente verknüpft mit einer antiferromagnetischen. Die magnetische Struktur ist dann nicht-kollinear und rührt von der starken magnetokristallinen Anisotropie her, die in derartigen Verbindungen mit niedriger Symmetrie eine Momentenrichtung bestimmt, die von einem Atom zum anderen unterschiedlich ist. Diese starke Anisotropie führt bei tiefer Temperatur zu einer schmalen Wand zwischen den magnetischen Domänen.

## 1. Introduction

The $R_2Pt$ compounds (R rare earth) crystallize in the orthorhombic $Ni_2Si$-type structure [1]. This structure can be built from trigonal prisms, where the corners are occupied by rare earth atoms and the center by a platinum atom. Platinum does not contribute to the magnetism of the compounds because the Stoner criterion for the onset of magnetism for 5d electrons is far from being satisfied. The magnetic interactions between rare earth atoms are of RKKY type and occur through polarization of the conduction band. Rare earth atoms lie in a very low symmetry site and because of the spin–orbit coupling the magneto-crystalline anisotropy is very high (when $L \neq 0$). The competition between these two effects (exchange and magnetocrystalline anisotropy) gives rise to unusual magnetization processes and to complex magnetic structures [2, 3].

In this paper we present the results of magnetization and suceptibility measurements together with neutron diffraction experiments performed on the $Tb_2Pt$ compound.

## 2. Experimental

The rare earth elements used were 99.9% pure and the platinum was 99.99% pure. Polycrystalline samples were induction melted in a cold crucible.

[1]) 25, Avenue des Martyrs, 166X, 38042 Grenoble Cédex, France.
[2]) Santander, Spain.
[3]) 85X, 38041 Grenoble Cédex, France.

Magnetic measurements between 4.2 and 300 K were performed at the S.N.C.I. (Service National des Champs Intenses, Grenoble) in fields up to 150 kOe. Magnetic structures were studied at the Laboratoire de Diffraction Neutronique du Centre d'Etudes Nucléaires de Grenoble (the neutron wavelength used on the diffraction spectrometer DN5 was 1.016 Å).

### 3. Crystallographic Structure

The $Ni_2Si$-type [4] crystallographic structure of $Tb_2Pt$ (Fig. 4) belongs to the Pnma ($D_{2h}^{16}$) space group. The lattice parameters of the orthorhombic cell which contains four formula units are: $a = 7.147$ Å, $b = 4.772$ Å, and $c = 8.763$ Å. All the atoms lie in the 4c site with $m(C_s)$ symmetry. The positions of the four atoms in this site are: (1) in $|x, \frac{1}{4}, 2|$, (2) in $|-x, \frac{3}{4}, -2|$, (3) in $|\frac{1}{2} - x, \frac{3}{4}, \frac{1}{2} + x|$, and (4) in $|\frac{1}{2} + x, \frac{1}{4}, \frac{1}{2} - z|$. From the intensities of neutron diffraction data performed above the ordering temperature, we have refined the atomic positions of the terbium and platinum atoms; these positions are presented in Table 1.

Table 1

Positions of the eight terbium and four platinum atoms in $Tb_2Pt$

| atoms | $x$ | $y$ | $z$ |
|---|---|---|---|
| Tb(1): 1, 2, 3, 4 | 0.868 | 0.25 | 0.073 |
| Tb(2): 5, 6, 7, 8 | 0.968 | 0.25 | 0.673 |
| Pt | 0.274 | 0.25 | 0.104 |

### 4. Magnetic Measurements

The thermal variation of the reciprocal susceptibility above 100 K is shown in Fig. 1. This variation follows a linear Curie-Weiss law which defines a paramagnetic Curie temperature of 99 K. The effective moment deduced from the slope of this linear variation is $9.56\mu_B$/Tb, in good agreement with the free ion value ($9.7\mu_B$). At 98 K, which is the Curie temperature, the suceptibility becomes very large; a spontaneous magnetization appears.

The field dependence of magnetization at various temperatures is shown in Fig. 2. At 20 K, as well as at 40 and 60 K, the curves indicate a typical ferromagnetic behaviour. However, above 8 kOe the magnetization which tends to saturate strongly depends on the applied field. This makes impossible the determination of spontaneous

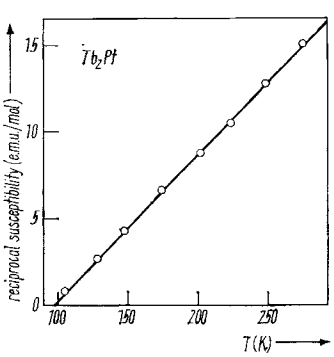


Fig. 1. Thermal variation of the reciprocal susceptibility of $Tb_2Pt$ in the paramagnetic range

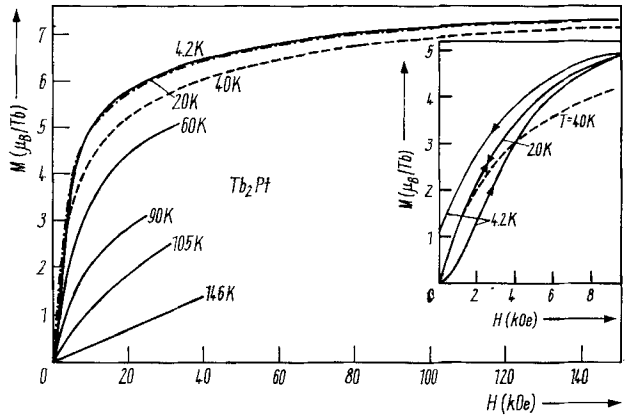


Fig. 2. First magnetization curves in $Tb_2Pt$ at different temperatures

magnetization. At 20 K, and in an applied field of 150 kOe the magnetization reaches $7.3\mu_B$/Tb, a value which is smaller than the free ion value ($9\mu_B$).

At 4.2 K the field dependence of magnetization is almost superimposed on that measured at 20 K. However, small shifts are observed especially in low fields. The enlargement of this region is shown in the insert of Fig. 2. The shape of the curve shows a smooth transition in the first magnetization curve together with a hysteresis loop. This behaviour, already observed in this type of intermetallic rare earth compounds, is attributed to the existence, between ferromagnetic domains, of narrow walls frozen by the anisotropy [5 to 9]. Indeed the magnetic domain wall thickness is essentially a function of the ratio between the exchange and magnetocrystalline anisotropy energies. At low temperature this ratio decreases and the wall thickness can be only a few interatomic distances. The applied field must be higher than a critical value to move these narrow walls which are frozen by the anisotropy: as observed in $Tb_2Pt$ the magnetization process is characterized by a transition in the first magnetization curve and by a hysteresis loop.

## 5. Magnetic Structure

The neutron diffraction patterns performed above and below the ordering temperature (120 and 4.2 K) are shown in Fig. 3. At 120 K the observed peaks are characteristic of the $Ni_2Si$-type crystallographic structure. Selection rules of the crystallographic Pnma space group are satisfied: the Bragg peaks $(h, k, 0)$ with $h = 2n + 1$ and $(0, k, l)$ with $k + l = 2n + 1$ do not appear. The calculated intensities with the Fermi length $b_{Tb} = 0.76 \times 10^{-12}$ cm and $b_{Pt} = 0.95 \times 10^{-12}$ cm are compared in Table 2 with the observed ones. The reliability factor is

$$R = \frac{\Sigma|I_{obs} - I_{cal}|}{\Sigma I_{obs}} = 3.4\% .$$

At 4.2 K the neutron diffraction pattern exhibits both an increase in the intensity of most of the nuclear reflections and the appearance of superstructure peaks, which can be indexed in the same orthorhombic cell. Especially the (100) and (001) reflections appear at low angle. The extinction conditions limiting the possible reflections of the Pnma space group are no longer valid. In order to determine the magnetic structure

Table 2
Observed and calculated neutron diffraction intensities at 120 and 4.2 K in $Tb_2Pt$

| | | 120 K | | | 4.2 K | | | |
|---|---|---|---|---|---|---|---|---|
| $h\ k\ l$ | $\theta$ | $I^N_{cal}$ | | $I^N_{obs}$ | $I^M_{cal}$ | | $(I^M + I^N)_{cal}$ | $I_{obs}$ |
| $\underline{0}\ \underline{0}\ \underline{1}$ | 3.32 | 0 | | 0 | 4.48 | | 4.48 | 4.7 |
| $\underline{1}\ \underline{0}\ \underline{0}$ | 4.07 | 0 | | 0 | 4.03 | | 4.03 | 3.4 |
| 1 0 1 | 5.26 | 0.01 | | 0 | 17.33 | | 17.34 | 24.8 |
| 0 0 2 | 6.66 | 2.37 | 6.06 | 10.1 | 21.06 | 97.16 | 103.22 | 102.7 |
| 0 1 1 | 6.96 | 3.69 | | | 76.10 | | | |
| 1 0 2 | 7.81 | 7.51 | | | 31.78 | | | |
| 1 1 1 | 8.07 | 12.35 | 22.13 | 27.8 | 122.81 | 200.38 | 222.51 | 220.8 |
| 2 0 0 | 8.17 | 2.27 | | | 36.27 | | | |
| $\underline{1}\ \underline{1}\ \underline{0}$ | 7.35 | 0 | | | 9.52 | | | |
| 2 0 1 | 8.83 | 3.55 | 3.55 | 6.2 | 7.46 | 34.64 | 38.19 | 41.9 |
| $\underline{0}\ \underline{1}\ \underline{2}$ | 9.05 | 0 | | | 27.18 | | | |
| 1 1 2 | 9.94 | 98.19 | | | 109.66 | | | |
| 2 1 0 | 10.23 | 113.61 | 211.8 | 214.4 | 45.19 | 170.83 | 382.63 | 435.6 |
| $\underline{0}\ \underline{0}\ \underline{3}$ | 10.01 | 0 | | | 15.98 | | | |
| 2 0 2 | 10.57 | 28.63 | | | 28.23 | | | |
| 2 1 1 | 10.76 | 183.63 | 263.58 | 268.1 | 115.35 | 152.82 | 416.40 | 420.5 |
| 1 0 3 | 10.82 | 51.32 | | | 9.24 | | | |
| 0 1 3 | 11.76 | 187.43 | | 189.3 | 83.04 | | 270.47 | 263.2 |
| 2 1 2 | 12.25 | 17.25 | | | 44.17 | | | |
| 0 2 0 | 12.30 | 193.59 | 260.29 | 258.3 | 75.18 | 136.87 | 397.16 | 380.4 |
| 1 1 3 | 12.47 | 49.45 | | | 13.79 | | | |
| $\underline{3}\ \underline{0}\ \underline{0}$ | 12.31 | 0 | | | 3.72 | | | |
| 3 0 1 | 12.77 | 15.59 | | | 11.84 | | | |
| 2 0 3 | 12.98 | 68.98 | 84.57 | 71.8 | 57.47 | 112.37 | 196.34 | 180.4 |
| $\underline{0}\ 2\ \underline{1}$ | 12.74 | 0 | | | 14.56 | | | |
| $\underline{1}\ \underline{2}\ \underline{0}$ | 12.95 | 0 | | | 28.50 | | | |
| 1 2 1 | 13.40 | 0 | 51.73 | 50.6 | 76.29 | 78.71 | 130.44 | 115.0 |
| 0 0 4 | 13.40 | 51.73 | | | 2.42 | | | |
| | | $R = 3.4\%$ | | | $R = 5.8\%$ | | | |

Underlined $(h\ k\ l)$'s correspond to selection rules of the crystallographic space group.

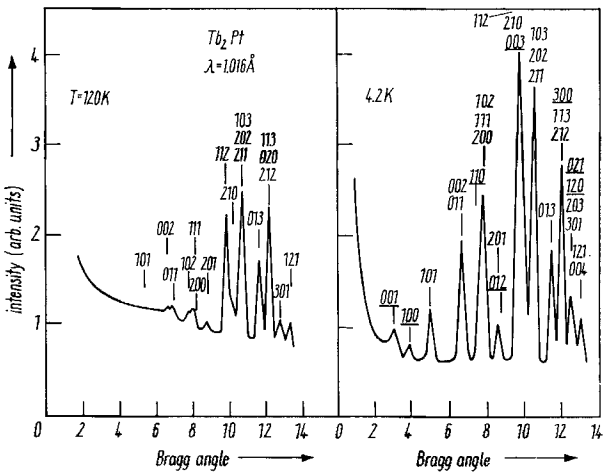


Fig. 3. $Tb_2Pt$ ($\lambda = 1.016$ Å): neutron diffraction patterns at 120 and 4.2 K. Underlined (*hkl*)'s correspond to selection rules of the crystallographic space group

we have used the macroscopic method of Bertaut [10]. This method allows one to obtain the linear combinations of magnetic moments which are the basis vectors of the irreducible representation associated with the space group corresponding to the propagation vector $\boldsymbol{K}$ of the magnetic cell. In our case, where $\boldsymbol{K} = \boldsymbol{0}$, these basis vectors are shown in Table 2.

The superstructure lines are characteristic of antiferromagnetic components which must be associated with ferromagnetic ones because of the existence of spontaneous magnetization. Then the irreducible representations associated with antiferromagnetic modes such as $(C_y)$, $(A_x, G_z)$, $(A_y)$, and $(G_x, A_z)$ cannot appear alone. Moreover a calculation of magnetic structure factors shows that $A$ and $G$ modes do not give any contribution to the (100) and (001) peaks which are accounted for only by the $C$ modes. Finally a refinement shows that the only way to account for the observed intensities is to consider a magnetic structure with basis vectors belonging to two different irreducible representations: $F_x, C_z$ belonging to $\Gamma_3$ for the Tb(1) atoms (1 to 4) and $C_x, F_z$, belonging to $\Gamma_2$ for the Tb(2) atoms (5 to 8).

The best agreement between the observed and calculated intensities (Table 3) was

Table 3

Irreducible representations and basis vectors of the space group Pnma associated with the propagation vector $\boldsymbol{K} = \boldsymbol{0}$

| representation | basis vectors | | |
|---|---|---|---|
| $\Gamma_1$ | — | $C_y$ | — |
| $\Gamma_2$ | $C_x$ | — | $F_x$ |
| $\Gamma_3$ | $F_x$ | — | $C_z$ |
| $\Gamma_4$ | — | $F_y$ | — |
| $\Gamma_5$ | $A_x$ | — | $G_z$ |
| $\Gamma_6$ | — | $G_y$ | — |
| $\Gamma_7$ | — | $A_y$ | — |
| $\Gamma_8$ | $G_x$ | — | $A_z$ |

$\boldsymbol{F} = \boldsymbol{M}_1 + \boldsymbol{M}_2 + \boldsymbol{M}_3 + \boldsymbol{M}_4$ ($\boldsymbol{M}_5 + \boldsymbol{M}_6 + \boldsymbol{M}_7 + \boldsymbol{M}_8$ for Tb(2)),
$\boldsymbol{G} = \boldsymbol{M}_1 - \boldsymbol{M}_2 + \boldsymbol{M}_3 - \boldsymbol{M}_4$,
$\boldsymbol{C} = \boldsymbol{M}_1 + \boldsymbol{M}_2 - \boldsymbol{M}_3 - \boldsymbol{M}_4$,
$\boldsymbol{A} = \boldsymbol{M}_1 - \boldsymbol{M}_2 - \boldsymbol{M}_3 + \boldsymbol{M}_4$.

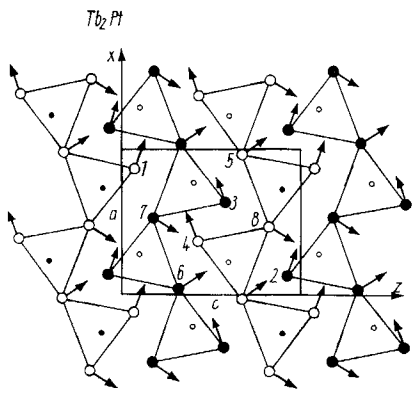


Fig. 4. Magnetic structure of $Tb_2Pt$. $y = 0.25$: ○ Tb, ∘ Pt; $y = 0.75$: ● Tb, • Pt

obtained with the same magnetic moment ($5.6\mu_B$) for Tb(1) and Tb(2) atoms. The characteristics of this model are presented in Table 4 and the resulting magnetic structure is shown in Fig. 4.

Table 4

Characteristics of the magnetic structure of $Tb_2Pt$

| atoms | basis vectors | $M_x(\mu_B)$ | $M_z(\mu_B)$ | $M(\mu_B)$ | angle with $0x$ axis |
|---|---|---|---|---|---|
| Tb(1) 1, 2, 3, 4 | $F_x$, $C_z$ | 5.2 | 2.0 | 5.6 | 20° |
| Tb(2) 5, 6, 7, 8 | $C_x$, $F_z$ | 3.0 | 4.7 | 5.6 | 57° |

## 6. Discussion

The magnetic structure of $Tb_2Pt$ is complex and non-collinear. Moments lie in the mirror plane perpendicular to the [010] direction. In the $(x, z)$ plane a ferromagnetic component is associated with an antiferromagnetic one, but the ferromagnetic components are not along the same axis for Tb(1) and Tb(2) atoms. This type of non-collinear magnetic structure is a general feature of the rare earth compounds with low symmetry [9]. Because of the difference of surroundings the magnetic atoms are divided into various sublattices with different easy magnetization directions. Then the complex magnetic structures result from a competition between the strong magnetocrystalline anisotropy and exchange interactions which are generally considered as isotropic.

For terbium atoms lying in the same site (Tb(1) or Tb(2)) the magnetic arrangement corresponds to basis vectors which belong to one irreducible representation ($\Gamma_3$ or $\Gamma_2$). This means that the coupling between these atoms takes place through a quadratic Hamiltonian. On the other hand, for Tb(1) and Tb(2) atoms the irreducible representations are different. As noticed by Bertaut [10] this may be interpreted as a decoupling or a coupling through a lower symmetry between the two types of terbium atoms. In terms of magnetic space group (Shubnikov) these $\Gamma_2$ and $\Gamma_3$ representations correspond to the Pn'm'a and Pnm'a' groups, respectively. The total magnetic space group is the monoclinic Pm' group which corresponds effectively to a lower symmetry.

In zero applied field the magnetic moment determined by neutron diffraction is the same for the two sublattices of Tb atoms and reaches only $5.6\mu_B$. This large reduction of the magnetic moment, as well as the strong anisotropy, is a result of the crystalline electric field effects.

The magnetization processes which exhibit a strong field dependence must correspond to an increase, as well as a progressive rotation, of the Tb magnetic moment. Indeed at 20 K when the variation of magnetization deviates from the demagnetizing field slope, magnetization is around $3.5\mu_B$/Tb whereas it reaches $7.3\mu_B$/Tb in 150 kOe.

Finally the strong anisotropy stabilizes at low temperature the narrow walls between magnetic domains. These walls, which are frozen, are responsible for the first magnetic curve observed at 4.2 K [5 to 9].

All these properties confirm the preponderant role of the crystal field effects in this compound with low symmetry.

## References

[1] J. Le Roy, J. M. Moreau, D. Paccard, and E. Parthe, Acta cryst. **B34**, 9 (1978).
[2] A. Castets, D. Gignoux, and J. C. Gomez-Sal, J. Solid State Chem. **31**, 197 (1980).
[3] D. Gignoux, J. Physique **35**, 455 (1974).
[4] K. Toman, Acta cryst. **5**, 329 (1952).
[5] H. Zijlstra, I.E.E.E. Trans. Magnetics **6**, 179 (1970).
[6] B. Barbara, C. Becle, R. Lemaire, and D. Paccard, C.R. Acad. Sci. (France) **B271**, 880 (1970).
[7] D. Gignoux and R. Lemaire, Solid State Commun. **14**, 877 (1974).
[8] D. Gignoux and J. S. Shah, Solid State Commun. **11**, 1709 (1972).
[9] B. Barbara, D. Gignoux, D. Givord, F. Givord, and R. Lemaire, Internat. J. Magnetism **4**, 77 (1973).
[10] E. F. Bertaut, Acta cryst. **A24**, 217 (1968).

*(Received March 18, 1982)*